

Aalborg Universitet



## Development of a Model-Based Approach to Capture Battery Parameter Degradation in Satellites

Knap, Vaclav; Beczkowski, Szymon Michal; Stroe, Daniel-Ioan

*Published in:*  
ECS Transactions

*DOI (link to publication from Publisher):*  
[10.1149/09901.0341ecst](https://doi.org/10.1149/09901.0341ecst)

*Publication date:*  
2020

*Document Version*  
Accepted author manuscript, peer reviewed version

[Link to publication from Aalborg University](#)

*Citation for published version (APA):*  
Knap, V., Beczkowski, S. M., & Stroe, D.-I. (2020). Development of a Model-Based Approach to Capture Battery Parameter Degradation in Satellites. *ECS Transactions*, 99(1), 341-350. <https://doi.org/10.1149/09901.0341ecst>

### General rights

Copyright and moral rights for the publications made accessible in the public portal are retained by the authors and/or other copyright owners and it is a condition of accessing publications that users recognise and abide by the legal requirements associated with these rights.

- Users may download and print one copy of any publication from the public portal for the purpose of private study or research.
- You may not further distribute the material or use it for any profit-making activity or commercial gain
- You may freely distribute the URL identifying the publication in the public portal -

### Take down policy

If you believe that this document breaches copyright please contact us at [vbn@aub.aau.dk](mailto:vbn@aub.aau.dk) providing details, and we will remove access to the work immediately and investigate your claim.



# Development of a Model-Based Approach to Capture Battery Parameter Degradation in Satellites

Vaclav Knap<sup>a,b,c</sup>, Szymon Bęczkowski<sup>c</sup> and Daniel-Ioan Stroe<sup>c</sup>

<sup>a</sup> GomSpace A/S, Aalborg, Denmark

<sup>b</sup> Faculty of Electrical Engineering, Czech Technical University in Prague,  
Czech Republic

<sup>c</sup> Department of Energy Technology, Aalborg University, Aalborg, Denmark

There is an increasing number of CubeSats being launched on the Earth's orbit. They are typically based on commercial off-the-shelf batteries that are not primarily designed for space applications. Thus, their actual degradation in this environment needs to be considered, compared to on-ground laboratory conditions. In this work, a model-based method is introduced for tracking the change in battery model parameters, including the battery capacity. The method is based on collected telemetry data and it covers specific and variable battery temperature conditions in CubeSats. However, it is shown that the method is sensitive to telemetry quality, regarding sample resolution and sample loss. Thus, the used settings could not determine battery degradation trends with high confidence. Nevertheless, steps for improvement were identified that shall increase the accuracy of the results in future work.

## Introduction

There is an increasing number of small satellites being launched into space. Amongst them, CubeSat solutions are getting popular due to their increasing capabilities, flexibility, and significantly lower price than 'classical' satellites. They are suitable to carry on dedicated missions with various purpose in fields of communications, earth observation, remote sensing, etc. Oftenly, they form constellations, in which they operate in a cooperative manner. Anyway, the first step is usually to perform an In-Orbit-Demonstration (IOD) mission, which serves for technology testing and as a proof of concept (1). That was also the case of GOMX-3 mission, which consisted of one 3U CubeSat built by GomSpace and launched in collaboration with ESA. Its purpose was to demonstrate the capabilities of nano-satellites in terms of attitude control, RF sensing, and high-speed downlink. Its mission lasted for about one year and the satellite was afterward successfully de-orbited (2),(3).

Batteries are crucial components, , which ensure that satellites have enough energy supply to conduct their mission and remain operation able, especially during eclipses, when there is no energy generated by solar panels. CubeSats use typically commercial off-the-shelf (COTS) battery cells. The advantage is that these cells are widely available for a relatively low price. However, as they are not primarily space dedicated, they have to be qualified for the launch and space environment. One of the harsh conditions, which batteries can experience at Low Earth Orbit (LEO), is for example rapid temperature

variations, especially in the case of a low thermal mass of the spacecraft and minimal or missing thermal management. Batteries have, even in these conditions, to provide sufficient performance and lifetime to successfully conduct the mission (4).

The paper introduces a battery model parametrization technique based on laboratory experiments. At first, the method is applied to a single battery cell, where it successfully captures the temperature dependence. Then, the technique is applied to a battery pack from an on-ground test. Finally, the method is used on telemetry data from GomX-3 in order to observe the parameters' trends over the satellite life during orbiting. Here, the challenge is the quality of telemetry data in terms of sample resolution and sample loss, since optimally constant sampling with one-second resolution is needed to match the laboratory testing level. The data used for system identification were pre-selected; only periods with a high amount of samples were used, and pre-processed, linear interpolation was used to obtain one-second resolution sampling. The obtained battery model parameters' values from satellite telemetry were in a range corresponding to laboratory tests, with two exceptions, which will be detailed in the paper.. Since the identified values were still significantly scattered, it was not possible to determine their degradation trends with high confidence. Nevertheless, the applied method seems promising and this work helped identified individual steps that should be leading to higher results quality and accuracy.

## **Experimental**

### **Satellite GOMX-3**

GOMX-3 was a 3U nano-satellite (1U is a size of a 10x10x10 cm cube) and its inner structure is shown in Fig. 1(a). Its mission had several goals, such as: 1) demonstrating three-axis attitude control with one-degree pointing accuracy; 2) monitoring aircrafts positions through ADS-B signal; 3) high speed (3 Mbps) downlink through X-band patch antenna; and 4) demonstrating new capabilities of software-defined radio payloads. The satellite was deployed on 5th October 2015 from the ISS, and it performed a planned re-entry into the Earth's atmosphere in October 2016. Since it was launched from the ISS, its inclination was 51.6° and the initial altitude around 400 km.

GOMX-3 was equipped with a BP4 battery pack, shown in Fig. 1(b). The BP4 uses four 18650 Li-ion cells with the nominal capacity of 2.6 Ah and the nominal voltage of 3.6 V. The cells were connected in a configuration 4S-1P, forming 14.4 V nominal voltage of the pack. The collected battery telemetry consisted of battery temperature, battery voltage, load current, and solar panel generated current.

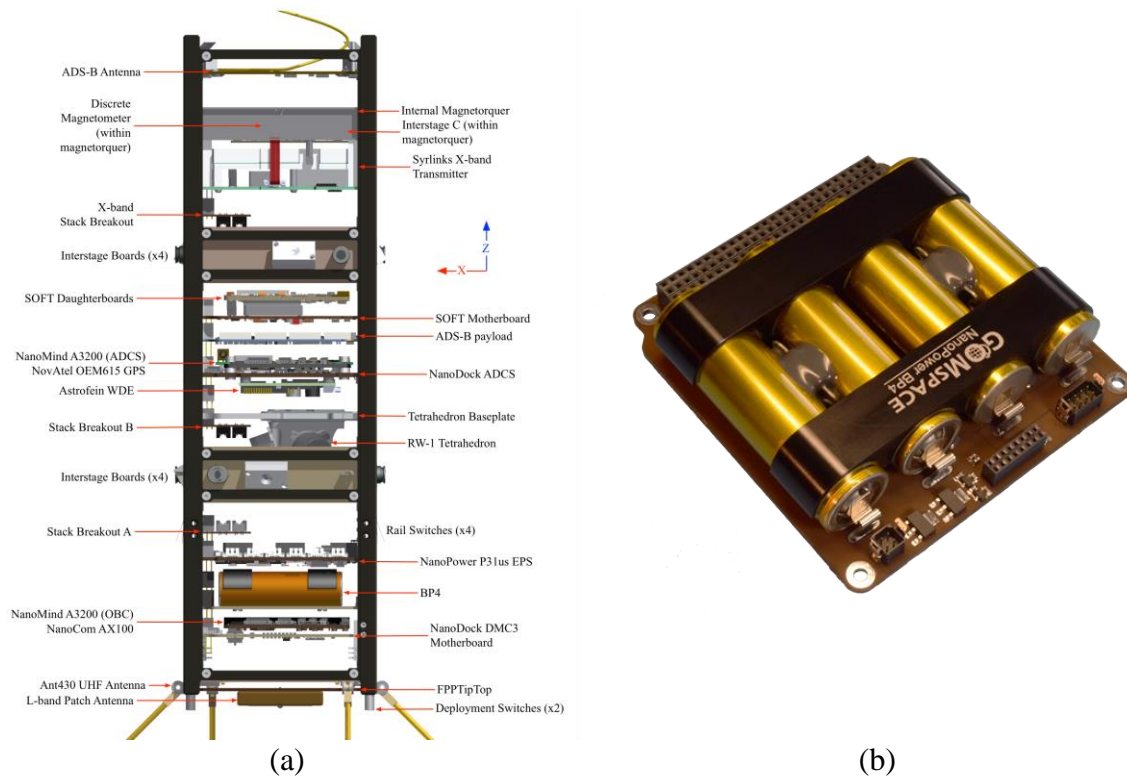


Figure 1. (a) GOMX-3 internal layout; (b) a BP4 battery pack. Copyright (2015), published with permission from GomSpace.

### Battery Ground Tests

Identical cells to the ones in the BP4 in GOMX-3 have been tested in the laboratory. They are GomSpace NanoPower Battery 2600mAh type cells with the minimum voltage of 2.75 V and the maximum voltage of 4.2 V. The experiments were performed on battery testers Digatron BTS 600 and Neware BTS 4000. The following tests were performed:

Open-Circuit Voltage (OCV) Test. A procedure of quasi-open-circuit voltage (qOCV) test was selected in this work to measure the battery OCV. The cell was completely charged and discharged with respect to the cell's voltage limits by a current of 0.25 A. The measurement was performed for 5, 15, 25, 35, and 45°C. The final OCV curves, dependent on state-of-charge (SOC), were determined as average curves from respective charging and discharging profiles. The measured voltage, current and temperature as an example of this measurement at 25°C are illustrated in Fig. 2(a).

Dynamic Discharge Performance (DDP) Test. The DDP test is applied to a fully charged cell. It consists of a repetitive sequence: discharging by 4 A for 10 seconds, discharging by 1 A for 20 seconds, charging by 1.25 A for 5 seconds, and 25 seconds relaxation. This sequence is repeated until the cell reaches the cut-off voltage (5). The DDP test is applied again for the five temperature levels. However, an adjustment is done for the test at 45°C due to the safety limits and the current levels are reduced to 1.6, 0.4 and 0.5 A, respectively. The measured curves from the performed DDP at 25°C are illustrated in Fig. 2(b).

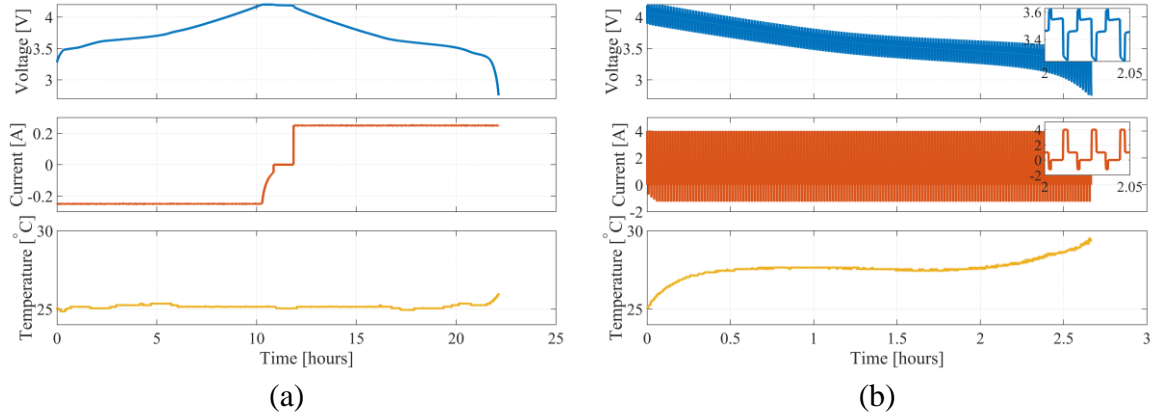


Figure 2. Examples of (a) an OCV test and (b) a DDP test performed at 25°C.

### Battery Modelling

An electrical circuit model (ECM) (6) was used to model the dynamic electrical behavior of a single battery cell. The model structure is shown in Fig. 3. The model in discrete time can be described by equations [1] – [3].

$$SOC[k+1] = SOC[k] - \frac{\Delta t}{Q_{dch}} i[k] \quad [1]$$

$$i_{R1}[k+1] = \exp\left(-\frac{\Delta t}{R_1 C_1}\right) i_{R1}[k] + \left(1 - \exp\left(-\frac{\Delta t}{R_1 C_1}\right)\right) i[k] \quad [2]$$

$$v[k] = OCV(SOC[k]) - R_1 i_{R1}[k] - R_0 i[k] \quad [3]$$

Where  $SOC$  stands for state-of-charge,  $\Delta t$  is the time step,  $Q_{dch}$  is the discharging cell capacity,  $i$  is the load current,  $i_{R1}$  is the current through the resistor  $R_1$ ,  $OCV$  is the open-circuit voltage and  $v$  is the battery terminal voltage.

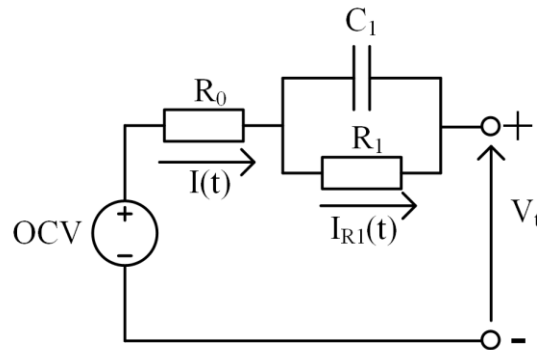


Figure 3. A structure of an equivalent circuit model (ECM) for a Li-ion battery cell.

Since the  $OCV$  for the model was already determined, it remains to identify the battery model parameters  $R_0$ ,  $R_1$  and  $C_1$ . Moreover, the discharging capacity term  $Q_{dch}$  is added amongst the parameters to be identified. Prediction-error minimization (PEM), proposed by Ljung (7), was used via MATLAB's System Identification Toolbox. The fit is evaluated using goodness of fit, which is computed as follows:

$$Goodness\ of\ fit = 100 \cdot \left(1 - \frac{\sqrt{(V_{meas} - V_{fit})^2}}{\sqrt{(V_{meas} - \bar{V}_{meas})^2}}\right) (\%) \quad [4]$$

For simplicity, it is assumed that the battery parameters other than OCV are independent of the SOC. However, since the battery experiences rapid and significant temperature changes in the satellite, it is necessary to account for the temperature dependency. Thus, at first, the model is parametrized individually for each temperature. The obtained values are shown in Table I.

**TABLE I.** The fitted ECM parameters from the DDP tests for individual temperatures.

DDP Temperature [°C]	$R_0$ [Ω]	$R_1$ [Ω]	$C_1$ [F]	$Q_{dch}$ [Ah]	Goodness of fit [%]
5	0.0886	0.0705	852.70	2.1745	90.23
15	0.0764	0.0527	923.51	2.3067	90.30
25	0.0697	0.0430	989.03	2.4124	90.59
35	0.0658	0.0452	1088.04	2.4981	91.28
45	0.0630	0.0612	1178.52	2.5534	97.11

The second step is to determine functions that capture the dependence of the parameters on temperature. According to Ref. (8), the Arrhenius law, presented in Eq. [5], was used to fit this dependence.

$$p(T) = p_{ref} \cdot \exp\left(\frac{E_a}{R} \left(\frac{1}{T} - \frac{1}{T_{ref}}\right)\right) \quad [5]$$

Where  $p$  stands for a battery model parameter (e.g.,  $R_0$ ,  $R_1$ ,  $C_1$  and  $Q_{dch}$ ),  $T$  is temperature in Kelvins,  $E_a$  is the activation energy,  $R$  is the universal gas constant and the subscript  $ref$  stands for a reference condition, which was considered a room temperature (25°C).

The individually-identified values and their fit, using Eq. [5], are shown in Fig. 4.

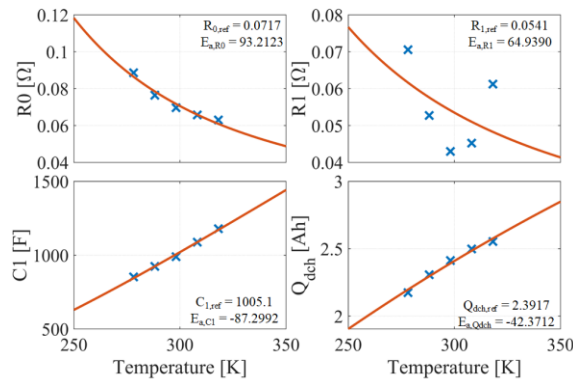


Figure 4. The obtained ECM parameters from the individual temperature DDP test fit and their temperature dependence fit via the Arrhenius law.

The last step in the determination of the ECM is to perform the PEM considering the functions describing the parameters' temperature dependence, as shown in Fig. 4, and all the DDP experiments at the same time. Thus, the PEM ensures to provide the best

solution for all considered temperatures and consistency among the parameters. The identified values are presented in Table II. In comparison to the values summarized in Table I., the goodness of fit decreased insignificantly.

**TABLE II.** The fitted temperature-dependent models for ECM parameters from coupled experiments.

	$R_0$	$R_1$	$C_1$	$Q_{dch}$
$p_{ref}$	0.0732 [ $\Omega$ ]	0.0536 [ $\Omega$ ]	985.1929 [F]	2.3596 [Ah]
$E_a$	100.0385 [kJ/mol]	99.8952 [kJ/mol]	-87.7106 [kJ/mol]	-47.4339 [kJ/mol]
Goodness of fit [%]	89.64 @ $T = 5^\circ\text{C}$ , 89.96 @ $T = 15^\circ\text{C}$ , 90.10 @ $T = 25^\circ\text{C}$ , 91.12 @ $T = 35^\circ\text{C}$ , 96.64 @ $T = 45^\circ\text{C}$			

A comparison of the measured and the simulated voltage for the DDP profile, at  $25^\circ\text{C}$ , is presented in Fig. 5. The model with the identified parameters can simulate the voltage response of the cell accurately over the region where resistance parameters are constant and less-dependent on the SOC. However, at the very low SOC, when the cell is nearly fully discharged, there is a SOC dependence, that is not captured with the actual model. Nevertheless, it is not expected, and neither it was observed for the satellite to operate in that SOC range. Thus, the established model shall be sufficient for further analysis.

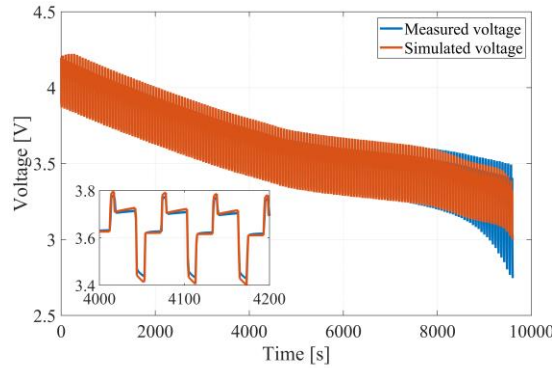


Figure 5. Measured and simulated voltage for the DDP profile at  $25^\circ\text{C}$ .

**Battery Pack Level.** The previous detail measurements and the modelling were performed at cell level. In the investigated battery pack, four cells are connected in series, and the voltage is only measured across all of them as a bulk. The voltage can be scaled down to a single cell. However, the influence of the conductive paths and interconnections will contribute to the extracted ECM parameters. During a ground test, a charge-discharge cycle (constant current-constant voltage (CC-CV) charging by 1.3 A to 4.2 V and 0.05 A, CC-CV discharging by 1.3 A to 3.0 V and 0.02 A, and charging again with the same conditions as before) at room temperature was performed on a new battery pack and the PEM was applied to obtain the battery model parameters scaled down to cell level from the battery pack. The goodness of fit was 90.13% and the identified parameters are shown in Table III. The found value for  $R_0$  in the pack was by an order of magnitude smaller than for the single cell, opposite to it,  $R_1$  was doubled. Considering the sum of the resistances (the total resistance  $R_T = R_0 + R_1$ ), the value obtained from the battery pack is  $0.1242 \Omega$ , and the value from the single cells is  $0.1268 \Omega$ . Thus, it can be considered that the total resistance is concurring in the single cell and the battery pack level. Moreover, CC-CV (dis)charge over the large, nearly the whole, SOC region is not a suitable current profile to capture varying battery voltage dynamics.

**TABLE III.** The fitted ECM parameters from a CC-CV charge-discharge test at BP4 at 25°C.

	$R_0$	$R_1$	$C_1$	$Q_{dch}$
$p_{ref}$	0.0087 [ $\Omega$ ]	0.1155 [ $\Omega$ ]	1104.2 [F]	2.5504 [Ah]
$E_a$	93.2111 [kJ/mol]	64.4660 [kJ/mol]	-120.8737 [kJ/mol]	-42.3720 [kJ/mol]

## Analysis

### Battery Modelling Approach Applied on the Telemetry Data

Since the battery modelling procedure allows us to extract battery model parameters from current, voltage, and temperature profiles, it can be applied to the telemetry data. The telemetry data was collected in periods, where there was a direct link between the satellite and the ground station, which resulted in a non-constant sampling and a partial data loss. Since the parametrization procedure was successfully tested on the laboratory data with a constant one-second resolution, the telemetry data shall be processed to be available in the same format. Unless there is a significant data loss, it has been found that linear interpolation can be applied on the telemetry data to obtain a one-second constant sampling step, while maintaining the original trends. The PEM is then applied to selected orbits to identify the parameters of the established model. An example of ‘a good fit’ and ‘a bad fit’, that is driven by the quality of data and of the interpolation, is illustrated in Fig. 6 (a) and (b), respectively.

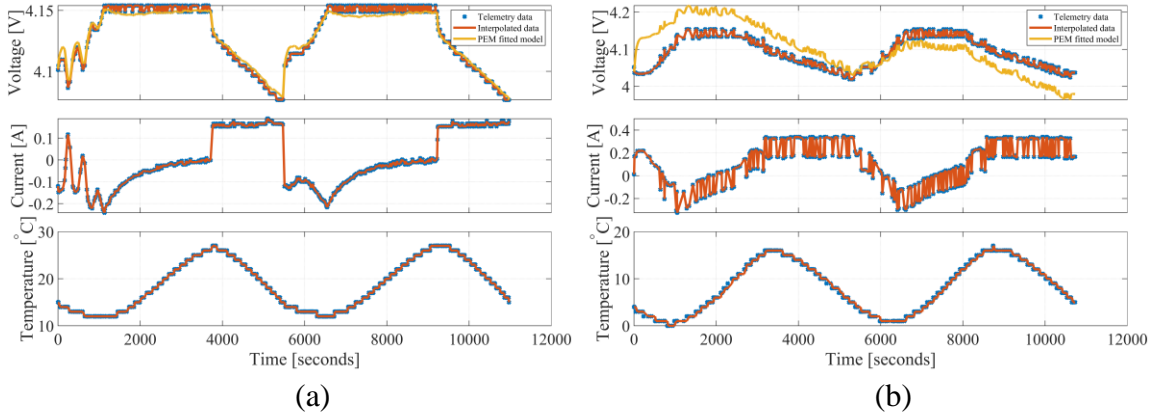


Figure 6. An example of an original telemetry data, their linear interpolation and the simulated voltage obtained from the model identified by PEM for (a) 2729 and 2730 orbit, with 92.98% goodness of fit, and for (b) 5637 and 5638 orbit with 38.56% goodness of fit.

Due to the relatively large amount of data and the time requirement for the fitting procedure, only 152 equally distributed orbit couples with a large number of data points were used. As it was demonstrated in Fig 6., the accuracy of the fit varied and the identified parameters were highly scattered. To reduce the noisiness, only the parameters obtained with the goodness of fit above 90% were considered and they are shown in Figure 7. The individual parameters are still somewhat scattered, but their variance decreased. In an attempt to capture the trend of the parameters, a linear fit was used, including depicting the confidence interval. Parameters  $R_0$  and  $R_1$  occur roughly in the range of the identified value from the on-ground tests of the single cell and the battery pack.  $C_1$  is approximately six times larger.  $Q$  is roughly in the range of the laboratory tests. Regarding the obtained activation energies, they are all similar to the laboratory

obtained values, except  $E_{a,R1}$ . The large variation of  $C_I$  can be explained from the collection of telemetry and data processing. The highest sample rating of the telemetry collection was 10 seconds. The collected data were then interpolated to one-second sampling for the system identification. Thus, certain battery voltage dynamics were not captured. Regarding  $E_{a,R1}$ , it is not clear, why it varies so significantly, because this parameter shall describe the variation of  $R_I$  due to temperature, and that shall not be so different from the laboratory tests. Due to too wide confidence intervals and sensitivity of trends according to selected orbits based on the identification error, no conclusions were made regarding the observed degradation trends. The considered approach requires a higher quality (high rate, no loss) telemetry sampling.

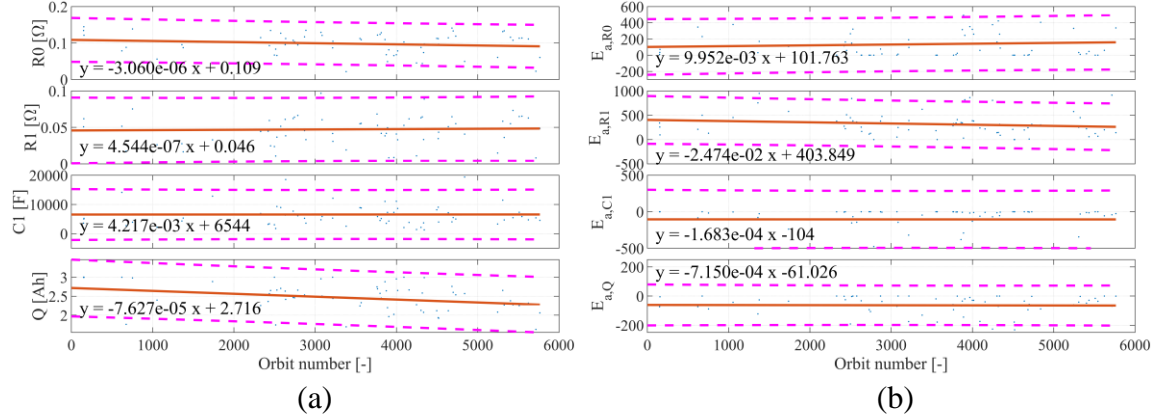


Figure 7. Identified battery model parameters over selected orbits with the goodness of fit above 90%. It is also shown their linear fit, including the 95% confidence interval. The activation energy ( $E_a$ ) unit is kJ/mol.

## Conclusion

A model-based approach for degradation detection of satellite batteries was introduced in this work. At first, a laboratory model of a single cell was developed, and the same system identification procedure was applied to a battery pack. Battery telemetry data was collected from GomX-3 Cubesat and it was further processed to be used for parameter identification. Selected orbit couples were then used to find the actual battery parameters, including the capacity; however, it was achieved with a varying accuracy. The found parameters' value appeared to be too noisy to draw any conclusions about their degradation trend. Despite that, the approach seems promising and as a part of future work, efforts will focus to increase the accuracy of the battery model, to increase the quality of telemetry data, and in general to increase confidence in the obtained trends, that it will be able to track and estimate state-of-health of the batteries in live satellites.

## Acknowledgments

This work was supported by Innovation Fund Denmark (Grant No: 8054-00027B).

## References

1. A. Camps, in *Satellites Missions and Technologies for Geosciences*, vol. i, p. 13, IntechOpen (2020).
2. D. Gerhardt, M. Bisgaard, L. Alminde, R. Walker, M. A. Fernandez, A. Latiri and J.-L. Issler, in *30th Annual AIAA/USU Conference on Small Satellites*, (2016).
3. J. A. Larsen, D. T. Gerhardt, M. Bisgaard, L. Alminde, R. Walker, M. Fernandez and J.-L. Issler, *4S Symp.*, 1–11 (2016).
4. V. Knap, L. K. Vestergaard and D.-I. Stroe, *Energies*, **13**, 4097 (2020).
5. G. Mulder, N. Omar, S. Pauwels, F. Leemans, B. Verbrugge, W. De Nijs, P. Van Den Bossche, D. Six and J. Van Mierlo, *J. Power Sources*, **196**, 10079–10087 (2011).
6. G. L. Plett, *Battery Management Systems*, v. 1., Artech House, (2015).
7. L. Ljung, *System Identification: Theory for the User*, 2nd ed., p. 640, Pearson, (1999).
8. Y. Troxler, B. Wu, M. Marinescu, V. Yufit, Y. Patel, A. J. Marquis, N. P. Brandon and G. J. Offer, *J. Power Sources*, **247**, 1018–1025 (2014).